Contract No. A1-030-32.

Supplementary Material Available: Tables I-VII, listing experimental data for the CH_3ONO-NO-alkane-air and Cl_2-NO-alkane-air irradiations (7 pages). Ordering information is available in any current masthead page.

Kinetics and Product Channels of the Reactions of HO_2 with O and H Atoms at 296 K

U. C. Sridharan, L. X. Qiu,† and F. Kaufman*

Department of Chemistry, University of Pittsburgh, Pittsburgh, Pennsylvania 15260 *(Received: June 15, 1982; In Final Form: July 30, 1982)*

Rate constants for the reactions HO_2 + O (1) and HO_2 + H (2) were measured in a discharge-flow apparatus fitted with back-to-back laser-induced fluorescence and vacuum UV resonance fluorescence detectors. The decays of [O] and [H] were monitored under conditions of large excess HO_2, generated by F + H_2O_2 and detected as OH after conversion with added excess NO. k_1 and k_2 were found to be $(5.4 \pm 0.9) \times 10^{-11}$ and $(7.4 \pm 1.2) \times 10^{-11}$ cm^3 s^{-1}, respectively. The branching ratios of (2), whose three sets of products are OH + OH (2a), H_2O + O (2b), and H_2 + O_2 (2c) were determined by reacting small, known concentrations of HO_2 with large excess of H and measuring the [OH] and [O] formed. They were found to be 0.87 ± 0.04, 0.04 ± 0.02, and 0.09 ± 0.045, respectively. These results are compared with published data and discussed in terms of the likely course of the molecular interactions.

Introduction

The chemistry of the HO_2 radical is of extraordinary importance in atmospheric processes as well as in combustion. HO_2 plays a major role in all phases of homogeneous chain reactions: in initiation steps where it is formed via H abstraction by O_2; in propagation or chain transfer steps, as, for example, in $HO_2 + O_3 \rightarrow OH + O_2 + O_2$, $OH + O_3 \rightarrow HO_2 + O_2$, or $HO_2 + NO \rightarrow OH + NO_2$; and in termination steps such as $OH + HO_2 \rightarrow H_2O + O_2$ or $H + HO_2 \rightarrow H_2 + O_2$. The two reactions investigated here

$$O + HO_2 \rightarrow OH + O_2 \qquad \Delta H^\circ_{298} = -52.7 \pm 1.0 \text{ kcal mol}^{-1} \quad (1)$$

$$H + HO_2 \rightarrow OH + OH \qquad \Delta H^\circ_{298} = -36.0 \pm 1.0 \text{ kcal mol}^{-1} \quad (2a)$$

$$\rightarrow H_2O + O \qquad \Delta H^\circ_{298} = -52.9 \pm 1.0 \text{ kcal mol}^{-1} \quad (2b)$$

$$\rightarrow H_2 + O_2 \qquad \Delta H^\circ_{298} = -54.6 \pm 1.0 \text{ kcal mol}^{-1} \quad (2c)$$

take part in many atmospheric processes. Their roles may be classified as odd oxygen removal, (1); HO_x radical propagation, (1) and (2a); partial chain termination, (1) and (2b); and full termination, (2c). These steps are important in the upper stratosphere and mesosphere, because fast atom-radical reactions are increasingly able to compete with three-body recombination at higher altitudes. They are also important in the detailed understanding and modeling of H_2-O_2 flame chemistry.

† Visiting scholar, Graduate School USTC, Academia Sinica, Peking, China.

The reactions of HO_2 with reactive species display surprising variety and unpredictability in their rate parameters. For example, reaction 3 is uncommonly fast,[1-3]

$$OH + HO_2 \rightarrow H_2O + O_2 \qquad \Delta H^\circ_{298} = -69.6 \pm 1.0 \text{ kcal mol}^{-1} \quad (3)$$

$k \sim (6\text{-}7) \times 10^{-11}$ cm^3 s^{-1}, and apparently exhibits a small pressure dependence,[4] strange as this may seem. The symmetrical reaction 4, on the other hand, is much slower,

$$HO_2 + HO_2 \rightarrow H_2O_2 + O_2 \qquad \Delta H^\circ_{298} = -37.6 \pm 1.5 \text{ kcal mol}^{-1} \quad (4)$$

and, in spite of much recent experimental work,[5] its basic mechanism is still in doubt. The reactions of HO_2 with atomic species are necessarily simpler in terms of their intermediates, but major uncertainties persist regarding both their rate constants and product channels, the latter particularly for (2). For (1), only one set of products, OH + O_2, is possible, but even there, one may visualize two different routes, H-atom transfer or O-atom transfer. This question may be resolved by oxygen isotope labeling but is unanswered now. Its rate constant, k_1, has been measured only recently,[6-9] the reported values ranging from

(1) Sridharan, U. C.; Qiu, L. X.; Kaufman, F. *J. Phys. Chem.* **1981**, *85*, 3361.
(2) Keyser, L. F. *J. Phys. Chem.* **1981**, *85*, 3667.
(3) Temps, F.; Wagner, H. Gg. *Ber. Bunsenges. Phys. Chem.* **1982**, *86*, 119.
(4) DeMore, W. B. *J. Phys. Chem.* **1982**, *86*, 121.
(5) Sander, S. P.; Peterson, M.; Watson, R. T.; Patrick, R. *J. Phys. Chem.* **1982**, *86*, 1236.
(6) Burrows, J. P.; Cliff, D. I.; Harris, G. N.; Thrush, B. A.; Wilkinson, J. P. T. *Proc. R. Soc. London, Ser. A* **1979**, *368*, 463.
(7) Hack, W.; Preuss, A. W.; Temps, F.; Wagner, H. Gg. *Ber. Bunsenges. Phys. Chem.* **1979**, *83*, 1275.
(8) Lii, R. R.; Sauer, M. C., Jr.; Gordon, S. *J. Phys. Chem.* **1980**, *84*, 817.
(9) Keyser, L. F. *J. Phys. Chem.* **1982**, *86*, 3439.

0022-3654/82/2086-4569$01.25/0

3×10^{-11} to 7×10^{-11} cm^3 s^{-1}. Most of these studies have been indirect, and some of their results were based on ratios of k_1 to other rate constants[6,7] whose values have since been revised. Keyser[9] has recently reported a direct measurement of k_1, including its temperature dependence, using the discharge-flow technique.

For (2), there have been three recent studies of its total rate constant.[10-12] The results of k_2 range from 4.6×10^{-11} to 6.0×10^{-11} cm^3 s^{-1}, but are dependent on other rate constants, because the experiments did not provide direct, kinetic data. The relative magnitude of the three product channels, (2a, 2b, and 2c), has been the subject of a large number of studies since 1963, most of them also indirect, with highly discordant results.[10,13-18] This is mainly due to two causes: insufficient and insensitive monitoring of reactive species (often only of a single species) with results based on modeling of multistep reaction schemes; and poor control of surface reactions. In the present work, we use the discharge-flow technique, monitor all major, reactive species with high sensitivity, reduce the role of surface reactions, and measure the desired processes directly.

Experimental Section

The apparatus has been described before.[1,19] The flow tube, 110 cm long, 2.54 cm i.d., is fitted with a concentric, movable, double injector tube. At its downstream end, a stainless steel fluorescence cell allows back-to-back measurement of radicals by laser-induced fluorescence (LIF) and of atoms by vacuum UV resonance fluorescence (VUVRF), 6 cm apart, with detection limits of $\sim 10^8$ cm^{-3} for OH (and HO_2 via chemical conversion to OH using excess NO) and $\sim 10^9$ for H and O atoms. The flow tube inner surface, injector tubes inner and outer surfaces, and detection cell were coated with Teflon or fluorocarbon wax as described earlier. Approximate values of the effective, pseudo-first-order surface removal rate constants, k_w, were ~ 4 s^{-1} for H and O, ~ 8 s^{-1} for OH, and ~ 2.5 s^{-1} for HO_2.

HO_2 was generated by the $F + H_2O_2$ reaction. F atoms were produced in a microwave discharge in the inner injector tube from small concentrations of CF_4 in He and reacted with measured excess of H_2O_2 in the outer injector.[1] H or O atoms were produced in microwave discharges from traces of H_2 or O_2 in He 125 cm upstream of the VUVRF detector. $[HO_2]$ was measured by conversion to OH with large excess [NO], $\sim 2 \times 10^{14}$ cm^{-3}, 5 cm upstream of the LIF detector, and calibrated by using the titration reaction $H + NO_2 \rightarrow OH + NO$ with excess [H], $\gtrsim 5 \times 10^{13}$ cm^{-3}, and measured NO_2 flows added 9 cm upstream of the LIF detector. [H] and [O] were monitored by VUVRF at 121.5 and 130.2 nm, respectively, and calibrated by quantitative conversion to OH with excess NO_2 (for [H]) and by the $N + NO \rightarrow N_2 + O$ reaction using excess [N] and measured NO addition (for [O]). The [O] calibration plot was linear to ±2% for $[O] \lesssim 1 \times 10^{11}$ cm^{-3}.

All experiments were done at room temperature, 296 ± 2 K, at flow tube pressures of ~2.5 torr of He, total flow velocities of ~1200 cm s^{-1}, with ~1/5 of the flow added through the 1.0-cm i.d. injector tube, and at typical concentrations of $[HO_2] \sim (2\text{–}20) \times 10^{11}$ cm^{-3}; $[H]_0$, $[O]_0 \sim (4\text{–}5) \times 10^{10}$ cm^{-3}; $[H_2O_2] \sim 8 \times 10^{12}$ cm^{-3}; $[NO] \sim 2 \times 10^{14}$ cm^{-3} (only for $[HO_2]$ measurement); and $[CF_4] \sim (1\text{–}10) \times 10^{13}$ cm^{-3} (for $F + H_2O_2$).

He (Linde, HP) was purified by passage over heated copper wool at ~700 K, followed by a molecular sieve (Type 4-A) trap at 77 K; NO (Matheson) was purified by slow passage through a column of ascarite at 1 atm pressure to remove higher oxides; NO_2 (Matheson) was purified by repeated freeze–pump–thaw cycles at 200 K; H_2O_2 (FMC Corp., 90% by weight) was concentrated and analyzed as before.[19]

Results and Discussion

Radical Concentration Measurements. An absolute calibration of $[HO_2]$ by the $H + NO_2$ reaction was carried out immediately after each $[HO_2]$ measurement (by NO conversion to OH). All [OH] measurements by LIF were corrected for OH loss by the reactions $OH + OH \rightarrow H_2O + O$, $k = 1.8 \times 10^{-12}$ cm^3 s^{-1}, and $O + OH \rightarrow O_2 + H$, $k = 3.3 \times 10^{-11}$ cm^3 s^{-1},[20] and by surface removal, $k_w \sim 8$ s^{-1}. These corrections typically totalled 5–8%. In the case of the $[HO_2]$ measurements, corrections for HO_2 surface removal were made as before,[19] but an additional, small correction term was added that had not been included in our recent work on the $OH + HO_2$ reaction.[1] The presence of excess [NO], $\sim 2 \times 10^{14}$ cm^{-3}, in the short HO_2-to-OH conversion zone slightly reduces [OH] in two ways: (a) by the three-body reaction $OH + NO + M \rightarrow HNO_2 + M$, calculated to produce a ~2.5% reduction; and by enhanced surface removal of OH due to NO (or second-order OH + NO reaction at the surface) estimated to produce another 2–3% reduction. The latter effect had been observed in earlier work,[21,22] and both corrections have recently been discussed and included by Keyser[9] in his work on reaction 1.

The validity of this correction, which is also applicable to our earlier work on k_3,[1] was confirmed experimentally in the following manner. Small [H] were converted to [OH] by adding excess NO_2 at a point 7 cm upstream of the LIF detector. Excess [NO], $\sim 2 \times 10^{14}$ cm^{-3}, was then added 2 cm further downstream, and the difference in the LIF signal of OH with and without added NO was measured. Twentytwo such experiments at $1 \times 10^{11} < [OH] < 20 \times 10^{11}$ cm^{-3} gave a decrease of (5 ± 1)% for [OH] in the presence of NO, in good agreement with the above-mentioned prediction.[21,22] This correction corresponds to an underestimate of $[HO_2]$ and therefore an overestimate of the published $OH + HO_2$ rate constant, $k_3 = k_3^I/[HO_2]$ where k_3^I was obtained from the pseudo-first-order OH decays with excess $[HO_2]$.

Rate Measurements. The experimental procedure for the measurement of total rate constants, k_1 and k_2, consisted of recording [O] or [H] VUVRF signals as function of the HO_2 injector position under conditions of excess HO_2, i.e., $5 < ([HO_2]/[O]_0$ or $[HO_2]/[H]_0) < 40$, and for five to six different $[HO_2]$. Pseudo-first-order rate constants, k_1^I or k_2^I, of 20–120 s^{-1} were obtained from semilog VUVRF intensity vs. injector position plots, Figures 1 and

(10) Hack, W.; Wagner, H. Gg.; Hoyermann, K. *Ber. Bunsenges. Phys. Chem.* **1978**, *82*, 713.
(11) Hack, W.; Preuss, A. W.; Wagner, H. Gg.; Hoyermann, K. *Ber. Bunsenges. Phys. Chem.* **1979**, *83*, 212.
(12) Thrush, B. A.; Wilkinson, J. P. T. *Chem. Phys. Lett.* **1981**, *84*, 17.
(13) Clyne, M. A. A.; Thrush, B. A. *Proc. R. Soc. London, Ser. A* **1963**, *275*, 559.
(14) Dodonov, A. F.; Lavroskaya, G. K.; Talroze, V. L. *Kinet. Katal.* **1969**, *10*, 701.
(15) Bennett, J. E.; Blackmore, D. R. *Symp. (Int.) Combust. [Proc.], 13th* **1971**, 57.
(16) Westenberg, A. A.; De Haas, N. *J. Phys. Chem.* **1972**, *76*, 1586.
(17) Baldwin, R. R.; Fuller, M. E.; Hillman, J. S.; Jackson, D.; Walker, R. W. *J. Chem. Soc., Faraday Trans. 1* **1974**, *70*, 635.
(18) Day, M. J.; Thompson, K.; Dixon-Lewis, G. *Symp. (Int.) Combust. [Proc.], 14th* **1973**, 47.
(19) Sridharan, U. C.; Reimann, B.; Kaufman, F. *J. Chem. Phys.* **1980**, *73*, 1286.
(20) JPL Publication No. 81-3, NASA, Jet Propulsion Laboratory, 1981.
(21) Anderson, J. G.; Margitan, J. J.; Kaufman, F. *J. Chem. Phys.* **1974**, *60*, 3310.
(22) Howard, C. J.; Evenson, K. M. *J. Chem. Phys.* **1974**, *61*, 1943.

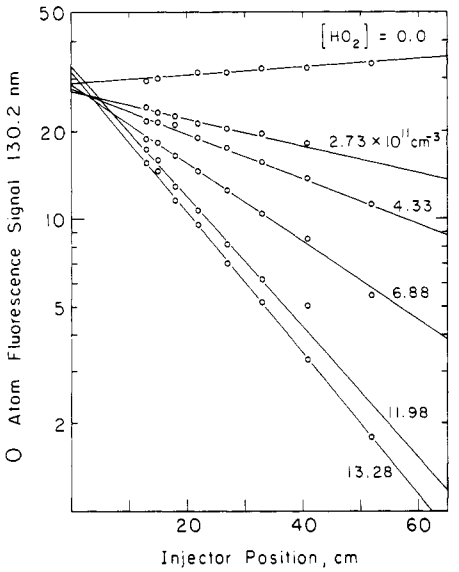

Figure 1. Reaction 1. O-atom decay plots for different $[HO_2]$.

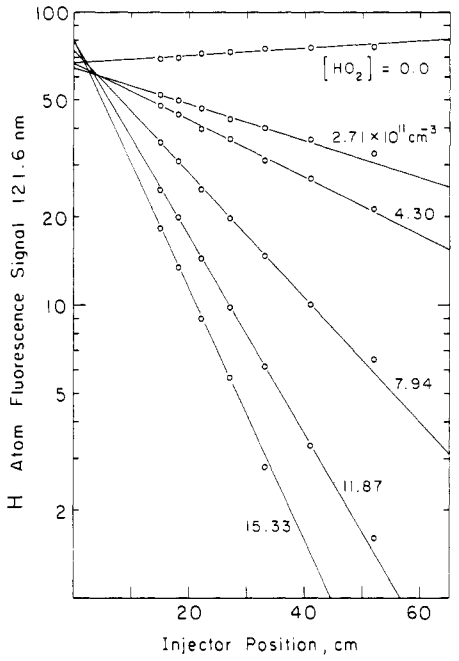

Figure 2. Reaction 2. H-atom decay plots for different $[HO_2]$.

2, that were linear over an order of magnitude change in [O] or [H]. The k^I's were corrected for axial diffusion, for HO_2 depletion at low $[HO_2]$ to $[O]_0$ or $[H]_0$ ratios, and for the injector effect[19] in the absence of added HO_2. The corrected k^I's were plotted vs. $[HO_2]$ in the usual manner, as shown in Figures 3 and 4. The desired second-order rate constants, $k_1 = k_1^I/[HO_2]$ and $k_2 = k_2^I/[HO_2]$, were obtained as the slopes of these linear plots from least-squares fits of the data. Figure 3 shows five sets of O + HO_2 rate experiments, each with five to six different $[HO_2]$, a total of 26 O-atom decays. The individual slopes, k_1, and intercepts are (4.3 ± 0.1) × 10^{-11} and 8.6 ± 1.4; (5.9 ± 0.3) × 10^{-11} and 0.1 ± 0.3; (5.4 ± 0.2) × 10^{-11} and 8.7 ± 3.1; (5.6 ± 0.2) × 10^{-11} and 5.0 ± 1.5; and (5.9 ± 0.3) × 10^{-11} cm^3 s^{-1} and −1.4 ± 2.3 s^{-1}, where the quoted uncertainties are the single standard deviations of the fits. Taking the average of these values and including estimated uncertainties of all input parameters gives k_1 = (5.4 ± 0.9) × 10^{-11} cm^3 s^{-1} at the 1σ error level. The average of the intercepts, 4.1 ± 2.2 s^{-1}, indicates that there are no complications due to surface reactions. Combining all 26 points

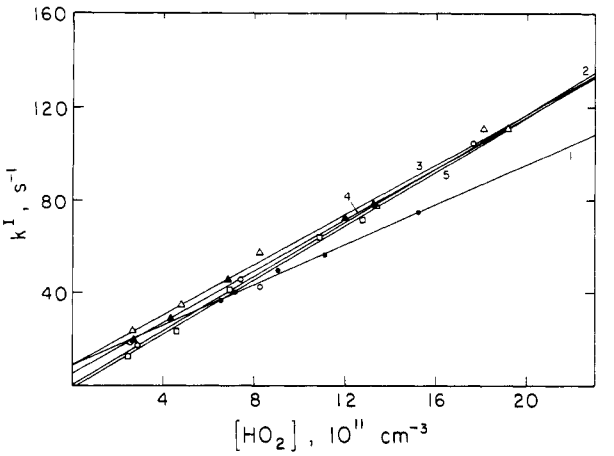

Figure 3. Plot of k_1^I vs. $[HO_2]$ for O + HO_2 reaction. Lines 1 through 5 are best fits for five separate experiments.

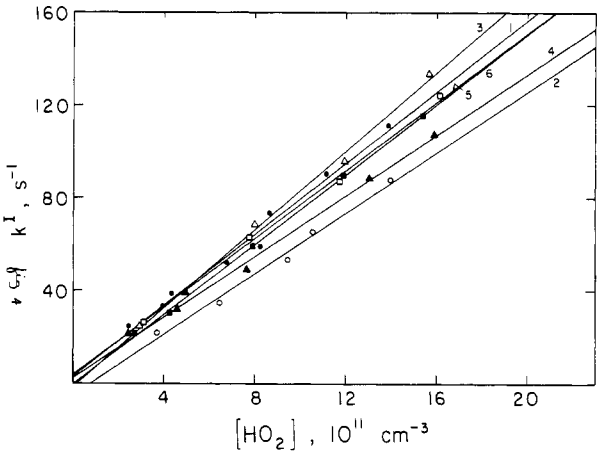

Figure 4. Plot of k_2^I vs. $[HO_2]$ for H + HO_2 reaction. Lines 1 through 6 are best fits for six separate experiments.

in a single k_1^I vs. $[HO_2]$ fit gives k_1 = (5.6 ± 0.9) × 10^{-11} cm^3 s^{-1} and 2.4 ± 2.0 s^{-1}.

Six sets of experiments for reaction 2, comprising 33 H-atom decays, are plotted in Figure 4. The slopes, k_2, and intercepts are (7.7 ± 0.4) × 10^{-11} and 2.8 ± 2.9; (6.6 ± 0.4) × 10^{-11} and −5.1 ± 3.6; (8.5 ± 0.3) × 10^{-11} and −1.5 ± 3.1; (6.6 ± 0.2) × 10^{-11} and 2.6 ± 2.4; (7.4 ± 0.3) × 10^{-11} and 3.4 ± 3.2; and (7.6 ± 0.1) × 10^{-11} cm^3 s^{-1} and −0.8 ± 1.3 s^{-1}. The averages, including other uncertaintites, give k_2 = (7.4 ± 1.2) × 10^{-11} cm^3 s^{-1} and an intercept of 0.2 ± 1.4 s^{-1}. Combining the 33 points in a single fit gives (7.3 ± 1.2) × 10^{-11} cm^3 s^{-1} and 1.1 ± 3.0 s^{-1}.

No correction was necessary for the slow reactions of O or H with H_2O_2 whose contributions to k_1^I and k_2^I are <0.5 s^{-1}. In all rate measurements, care was taken to make all necessary corrections for diffusion, viscosity, and surface effects in the usual manner.[1,19]

Product Channel Measurements. Although reaction 1 has only a single product channel, OH + O_2, several experiments were performed to confirm the formation and subsequent decay of OH under typical experimental conditions. A simplified kinetics analysis includes OH formation by reaction 1 and removal by reaction 3, by OH + H_2O_2 → HO_2 + H_2O (5), and by surface recombination, k_w^{OH}. In the plug flow approximation

$$\bar{v}\frac{d[OH]}{dx} = k_1^I[O] - k_L^I[OH]$$

where $\bar{v}$ is the average flow velocity, $k_1^I = k_1[HO_2]$, and $k_L^I = k_3[HO_2] + k_5[H_2O_2] + k_w^{OH}$. At the position of $[OH]_{max}$, $k_1^I = k_L^I[OH]_{max}/[O]_{max}$ and $k_1 = k_L^I[OH)_{max}/([O]_{max}$.

$[HO_2]$) where $[O]_{max}$ is the O-atom concentration at the position of $[OH]_{max}$. Since the VUVRF detector is 6 cm downstream of the LIF detector, $[O]_{max}$ was measured by moving the HO_2 injector 6 cm downstream after locating and measuring $[OH]_{max}$.

It should be emphasized that this method of determining k_1 is much less accurate than the direct measurement of O-atom decays since it involves locating the Local [OH] maximum and measuring the absolute O-atom concentration at a point where it is changing rapidly. Nevertheless, the experiment is useful, because it confirms the reaction stoichiometry. In three such experiments with excess $[HO_2] = 10.4$, 7.4, and 4.9×10^{11} cm^{-3} and $k_L^I = 121$, 100, and 82 s^{-1}, respectively, setting $k_3 = 7.1 \times 10^{-11}$ (slightly corrected value, see below) and $k_5 = 1.7 \times 10^{-12}$ cm^3 s^{-1},[19] $[OH]_{max}$ and $[O]_{max}$ were measured to be 1.2×10^{10} and 2.8×10^{10}, 1.0×10^{10} and 3.1×10^{10}, and 1.2×10^{10} and 2.7×10^{10} cm^{-3}, respectively. This gives $k_1 = 5.0 \times 10^{-11}$, 4.3×10^{-11}, and 7.4×10^{-11} cm^3 s^{-1} for the three experiments, i.e., $(5.6 \pm 2.0) \times 10^{-11}$, in very good agreement with the more accurate value reported in the previous section and thereby confirming the reaction stoichiometry.

For reaction 2, there are three different, energetically allowed product channels whose magnitudes need to be determined. In this study, the OH produced in (2a) and the O atoms produced in (2b) can be measured accurately, but the $H_2 + O_2$ produced in (2c) cannot. Since HO_2 reacts rapidly with both OH and O, the branching ratio experiments were carried out by adding small, measured concentrations of HO_2, $\sim 1 \times 10^{11}$ to 6×10^{11} cm^{-3}, to large excess [H], $\sim 10^{14}$ cm^{-3}, so that reaction 1 was complete in <1 ms. The movable injector was placed 5 cm upstream of the LIF port where it served both as the HO_2 source and, by measured addition of NO_2, as the NO_2 source in the absolute calibration of [OH]. The products, OH and O, could thus be measured accurately with little interference from fast, secondary reactions.

The branching ratio for (2a), $R_{2a} \equiv k_{2a}/k_2$, was determined as $[OH]_{corr}/(2[HO_2])$, where $[OH]_{corr}$ is the measured [OH] corrected for the following, small perturbations: (a) a contribution to [OH] of 1–7% due to the slow reaction $H + H_2O_2 \rightarrow OH + H_2O$ (6) that was subtracted from the measured [OH]; this was determined experimetnally for each [OH] measurement by shutting off the CF_4 discharge and monitoring the background [OH] due to $H + H_2O_2$. Interestingly, this correction term, as measured here, is about an order of magnitude smaller than that calculated on the basis of the rate constant $k_6 = 5.3 \times 10^{-14}$ cm^3 s^{-1} reported by Klemm et al.[23] but is in qualitative agreement with earlier studies.[24] (b) The $OH + H_2O_2$ reaction produces HO_2 to the extent of 6–7% under present experimental conditions. The HO_2 reacts rapidly with the excess H to produce more OH than was present originally because of the high branchng ratio (~0.9) of reaction 2a as shown below. This results in an overestimate of [OH] by 5–6%. This correction term, too, was monitored experimentally for each [OH] and $[HO_2]$ measurement by producing equivalent [OH] via $H + NO_2$ in excess [H] and recording the LIF signal for OH both with and without added H_2O_2; (c) the small corrections for the OH + OH reaction and for surface removal, applied as in the rate experiments, result in an underestimate of [OH] by ~5%. The $[HO_2]$ measurement by NO conversion to OH was carried out, and the results corrected as described above. In Table I are given 34 corrected values of R_{2a} at different $[HO_2]$.

TABLE I: $H + HO_2$ Branching Ratio Measurements

$10^{-11} \times [HO_2]$, cm^{-3}	R_{2a}	R_{2b}	$10^{-11} \times [HO_2]$, cm^{-3}	R_{2a}	R_{2b}
1.35	0.90		3.88	0.94	0.05
2.09	0.92		1.54	0.92	0.05
2.33	0.87		2.23	0.92	0.03
3.33	0.92		1.31	0.91	0.05
4.73	0.92		2.80	0.91	0.03
5.25	0.92		5.05	0.92	0.04
4.59	0.83	0.04	1.57	0.84	0.03
2.31	0.85	0.05	2.55	0.85	0.02
1.36	0.85	0.06	3.68	0.82	0.04
2.90	0.86	0.07	5.25	0.84	0.03
4.19	0.84	0.08	5.88	0.82	0.03
5.69	0.84	0.07	5.98	0.81	0.04
1.77	0.86	0.03	4.59	0.83	0.04
0.61	0.82	0.04	3.03	0.85	0.03
1.22	0.90	0.03	1.05	0.84	0.02
2.37	0.89	0.04	1.98	0.87	0.02
3.28	0.89	0.05	4.61	0.87	0.05
			av	0.87 ± 0.04	0.04 ± 0.02

In 28 of these experiments, the small amount of O-atom product was also monitored. Here, the correction terms are large in relative magnitude, although small in absolute amount. They include (a) the independent O-atom source term due to $OH + OH \rightarrow H_2O + O$ that must be subtracted from the measured [O], and (b) the O-atom depletion term by $O + OH \rightarrow O_2 + H$ that is added to the measured [O]. The contribution due to (a) was determined by generating equivalent OH concentrations independently by $H + NO_2$, adding $[H_2O_2]$ equal to that of the normal $H + HO_2$ experiments, and measuring the O atoms produced. This correction reduces the measured [O] by about 60–80%. The second correction, the reduction of the measured [O] due to the OH + O reaction at the measured [OH], was calculated based on its known rate constant,[20] $k = 3.3 \times 10^{-11}$ cm^3 s^{-1}, and amounted to increases of from 6–30%, depending on the experimental [OH]. In the calculation of $R_{2b} = k_{2b}/k_2 = [O]_{corr}/[HO_2]$ and in that of R_{2a}, all of the usual, small corrections for $[HO_2]$ were also applied, as described in the earlier section. The corrected values of R_{2b} are listed in Table I.

The results for the three branching ratios are $R_{2a} = 0.87 \pm 0.04$, $R_{2b} = 0.04 \pm 0.02$, and, by difference, $R_{2c} = 0.09 \pm 0.045$, where the uncertainties of R_{2a} and R_{2b} are single standard deviations about their mean, not of the mean. The latter is smaller by about a factor of five. The large uncertainty of R_{2b} includes the fact that it is obtained as the small difference of two quantities whose individual random errors are 10–15% each. Since R_{2a} is the ratio of concentrations measured in the same experiment in an identical manner, i.e., as OH by LIF, no other uncertainties need be considered. R_{2b} is very small, and its standard deviation is so large that other uncertainties are relatively insignificant. The three rate constants are, therefore, $k_{2a} = (6.4 \pm 1.0) \times 10^{-11}$, $k_{2b} = (3.0 \pm 1.5) \times 10^{-12}$, and $k_{2c} = (6.7 \pm 3.4) \times 10^{-12}$ cm^3 s^{-1}. It should be noted that if the standard deviations of the mean are used, $R_{2a} = 0.87 \pm 0.01$, $R_{2b} = 0.04 \pm 0.01$, the uncertainty of R_{2c} would be reduced to ±0.015, and the rate constants k_{2b} and k_{2c} would be reported as $(3.0 \pm 0.9) \times 10^{-12}$ and $(6.7 \pm 1.5) \times 10^{-12}$ cm^3 s^{-1}, respectively. The highly exothermic reaction 2a is likely to lead to vibrational excitation of the newly formed OH, and one may therefore need to consider interference effects due to the fact that $OH(v) + OH$ is probably faster than its ground-state counterpart and would increase the rate of O-atom formation. However,

(23) Klemm, R. B.; Payne, W. A.; Stief, L. J. *Int. J. Chem. Kinet. Symp.* **1975**, 61.
(24) Albers, E. A.; Hoyermann, K.; Wagner, H. Gg.; Wolfrum, J. *Symp. (Int.) Combust. [Proc.], 13th* **1971**, 81. Gorse, R. A.; Volman, D. H. *J. Photochem.* **1972**, *1*, 1. **1974**, *3*, 115.

TABLE II: Summary of Product Channel Branching Ratios for Reaction 2 near 300 K

ref	method	R_{2a}	R_{2b}	R_{2c}
13	H + O_2 + M, H_2O analysis			0.33 ± 0.12
14	H + O_2 + M, MS	0.05	0.52	0.43
15	H + O_2 + H_2, ESR			0.43
16	H + O_2 + M, ESR	0.27	0.11	0.62
10	H + O_2 + M, ESR	0.69	≤0.02	0.29
this work	H + HO_2, LIF, VUVRF	0.87 ± 0.04	0.04 ± 0.02	0.09 ± 0.045

the large excess [H] will relax OH(v) extremely rapidly, since $k \sim 3 \times 10^{-10}$ cm^3 s^{-1}.[25] Effective first-order energy transfer rate constants of $\gtrsim 10^4$ s^{-1} therefore ensure the rapid removal of OH(v).

Comparison with Other Results

Our value of $k_1 = (5.4 \pm 0.9) \times 10^{-11}$ cm^3 s^{-1} is in very good agreement with Keyser's[9] result of $(6.1 \pm 0.6) \times 10^{-11}$ based on a similar, direct experimental method. It is in poor agreement with the results of Burrows et al.,[6] $(3.3 \pm 1.0) \times 10^{-11}$, and of Hack et al.,[7] $(3.1 \pm 1.0) \times 10^{-11}$ cm^3 s^{-1}, for reasons that were discussed by Keyser[9] and need not be repeated here. Lii et al.'s[8] $(7 \pm 2) \times 10^{-11}$ is based on computer modeling of a multistep mechanism whose low sensitivity to changes in k_1 does not support their narrow uncertainty limits.[9] As in the case of reactions 3 and 5, the desired rate constant is best obtained in direct experiments that minimize interference due to other processes.

For reaction 2, there have been three published measurements of the total rate constant, k_2, to be compared with our value of $(7.4 \pm 1.2) \times 10^{-11}$ cm^3 s^{-1}: Hack et al.[10] monitored [H], [O], and [OH] in the recombination reaction H + O_2 + M, using electron spin resonance, i.e., at fairly low detection sensitivity, and reported $k_2 = (6 \pm 1.7) \times 10^{-11}$ cm^3 s^{-1} as well as branching ratios of 0.69, ≤0.02, and 0.29, for R_{2a}, R_{2b}, and R_{2c}. A more recent study by Hack et al.[11] which used laser magnetic resonance detection of OH and HO_2 and generated HO_2 either by H + O_2 + M or by F + H_2O_2 gave $(6 \pm 2) \times 10^{-11}$ from steady-state measurements and $(4.6 \pm 1.0) \times 10^{-11}$ from [HO_2] decays with and without added H. The authors preferred the latter value as the more directly measured one, but it, too, required computer simulation of a 12-step mechanism that included fast surface recombination of OH as well as other rate parameters whose values have since been revised. A brief, recent paper by Thrush and Wilkinson[12] reports HO_2 steady-state concentration measurements by laser magnetic resonance of the H + O_2 + M reaction system under conditions of very fast OH surface recombination. This is combined with an uncertain literature value for k_{H+O_2+M} to yield $k_2 = (5.0 \pm 1.3) \times 10^{-11}$ cm^3 s^{-1}. Not enough information is presented to allow an evaluation of the study's real uncertainties. The use of reactive surfaces introduces serious problems of reproducibility and of radical transport effects and should be avoided.

Table II lists all published values of relative branching ratios for (2) near room temperature. With exception of the work of Hack et al.[10] there is total lack of agreement. A detailed a posteriori analysis of the early studies is unwarranted. Suffice to say that they suffer in varying degree from lack of detection sensitivity, from incomplete monitoring of the several atom or radical species, from poorly characterized surface effects, and from uncertain assumptions regarding the complicated reaction schemes. The agreement with Hack et al.[10] is quite good on the two measured branches, (2a) and (2b), but their value for R_{2a}, although only ~20% lower than ours, leaves the "dark" channel, R_{2c}, more than a factor of three larger than ours.

From measurements of the second explosion limit of H_2 + O_2 mixtures at low [O_2] at 773 K, Baldwin et al.[17] have calculated a value of ~0.15 for R_{2c}. Dixon-Lewis and co-workers[18] have analyzed fuel-rich H_2 + O_2 flames and have reported values of 0.79, 0.08, and 0.13 for R_{2a}, R_{2b}, and R_{2c} near 1100 K. Combining these values for R_{2c} with the then available room temperature values, which were in error, these authors calculated an activation energy of (2a), E_{2a}, about 1.7–2.2 kcal mol^{-1} higher than that of (2c) and were forced to propose a very large preexponential factor of 5×10^{-10} cm^3 s^{-1} for (2a). This difficulty appears now to be resolved, since R_a is much larger at 296 K than reported earlier. The branching ratio, R_{2a}, may, in fact, have a small, negative and R_{2c} a small, positive temperature dependence, but the combination of results from such widely different methods and over such wide temperature ranges is somewhat suspect. The temperature dependence of reactions 1–3 is therefore under investigation in our laboratory.

Discussion

Our present findings tend to lessen the discrepancy between observation and model calculations of mesospheric O and O_3.[26] The larger value for k_1 and the smaller one for k_{2c} both increase the rate of the catalytic removal of odd oxygen; the former accelerates the catalytic cycle, and the latter lowers the removal rate for HO_x catalyst species.

Reactions 1 and 2 are seen to be fast atom–radical steps, and one may ask whether their detailed course may be rationalized on the basis of their rate constants, branching ratios, and comparison with similar processes. Lee and Howard[27] have recently investigated the reaction

$$Cl + HO_2 \rightarrow HCl + O_2 \qquad \Delta H^\circ_{298} = -53.6 \pm 1.0 \text{ kcal mol}^{-1} \quad (6a)$$

$$\rightarrow ClO + OH \qquad \Delta H^\circ_{298} = +2.2 \pm 1.0 \text{ kcal mol}^{-1} \quad (6b)$$

using laser magnetic resonance detection of HO_2, OH, and ClO. The total rate constant, k_6, was found to be nearly temperature independent, $(4.2 \pm 0.7) \times 10^{-11}$ cm^3 s^{-1}. The minor channel, (6b), has a positive temperature dependence, $k_{6b} = (4.1 \pm 0.8) \times 10^{-11} \exp[-(450 \pm 60)/T]$, as it must, in view of its endothermicity, whereas the major channel has a slight, negative dependence, $k_{6a} = (1.8 \pm 0.5) \times 10^{-11} \exp[(170 \pm 80)/T]$ cm^3 s^{-1}. Shortly before these accurate experimental results were published, Weissman et al.[28] had proposed that the reaction proceeded by way of an HOO··Cl intermediate complex, because its rate constant was too large for a tight, H-atom transfer transition state of the type Cl··HO_2. If the same, simple model is applied to the O + HO_2 reaction, one arrives at a similar conclusion, i.e., if the O··HO_2 bond is extended by only

(25) Spencer, J. E.; Glass, G. P. *Chem. Phys.* **1976**, *15*, 35.

(26) Allen, M.; Yung, Y. L.; Waters, J. W. *J. Geophys. Res.* **1981**, *86*, 3617.

(27) Lee, Y.-P.; Howard, C. J. *J. Chem. Phys.* **1982**, *77*, 756.

(28) Weissman, M.; Shum, L. G. S.; Heneghan, S. P.; Benson, S. W. *J. Phys. Chem.* **1981**, *85*, 2863.

0.4–0.5 Å, then one-half of the hard-sphere collision frequency of O with the H end of HO_2 gives an upper limit of about 2.3×10^{-11} cm^3 s^{-1} whereas the measured rate constant, k_1, is 5.4×10^{-11} cm^3 s^{-1}. Unless one were to propose an unreasonably large O··HO_2 bond extension, by ~1.1–1.2 Å beyond the normal O–H bond length of 0.97 Å, the experimental result suggests an HOO··O intermediate complex. Although this argument does not hold for larger radicals where radical–radical reactions are often faster than equivalent radical–molecule reactions, it is more likely to hold for small species where the abstraction is faster to begin with and where a large increase in its rate constant is harder to rationalize.

If the HO_3 complex decays by HO··OO cleavage, the product OH should be vibrationally cold, whereas the H-abstraction route should result in the formation of vibrationally excited OH. For reaction 6, the equivalent HO··OCl cleavage is endothermic and leads to the minor channel, (6b), but with a large A value of 4.1×10^{-11}. The major channel, (6a), may occur either via H abstraction or via four-center decay of $HOOCl^{\dagger}$. For the O + HO_2 reaction, isotope labeling and infrared chemiluminescence experiments may provide the information needed to resolve this question, but they will be complicated by interference due to secondary reactions.

For reaction 2, the simple model[28] gives an upper bound of about 6×10^{-11} cm^3 s^{-1}, only a little smaller than our experimental 7.4×10^{-11} cm^3 s^{-1}. The large branching ratio for the OH + OH product channel is consistent with the formation of an energy-rich HOO··H, i.e., an $H_2O_2^{\dagger}$ intermediate that would be formed via a long-range interaction similar to that used to describe radical recombination. The second largest channel, (2c), may involve either a direct H abstraction or the four-center decay of $H_2O_2^{\dagger}$. Considering its small rate constant of $\sim 7 \times 10^{-12}$ cm^3 s^{-1}, one needs to postulate the existence of a small activation barrier in spite of its large exothermicity, if (2c) occurs via H abstraction, i.e., $E_{2c} \sim 1$ kcal mol^{-1}. On the other hand, if (2c) occurs via four-center decay, its branching ratio should show no temperature dependence. We hope to resolve this question by our planned measurement of the temperature dependence of the (2a) and (2b) branching ratios. The small magnitude of R_{2b} and k_{2b} suggests the existence of an energy barrier for the attack of H on the middle O atom.

Corrected Value of the Rate Constant, k_3, for OH + $HO_2 \rightarrow H_2O + O_2$

As was described in the Experimental Section, the HO_2 concentrations, measured by conversion to OH with excess NO, had to be corrected upward by 5 ± 1% for the homogeneous and heterogeneous effect of NO. This correction lowers our earlier value[1] of k_3 from $(7.5 \pm 1.2) \times 10^{-11}$ to $(7.1 \pm 1.2) \times 10^{-11}$ cm^3 s^{-1} and improves the agreement with the values of $(6.4 \pm 1.5) \times 10^{-11}$ by Keyser[2] and $(6.7 \pm 2.3) \times 10^{-11}$ by Temps and Wagner.[3]

Acknowledgment. This work was supported by the National Aeronautics and Space Administration under Grant NGR 39 011 161.

Study of the Surface Composition of Zeolites by Fast Atom Bombardment Mass Spectrometry

John Dwyer,* Frank R. Fitch, Guanlin Qin,† and John C. Vickerman

Department of Chemistry, University of Manchester Institute of Science and Technology, Manchester M60 1QD, United Kingdom

(Received: February 16, 1982; In Final Form: July 20, 1982)

The surface composition and depth profiles of zeolites A, X, Y, mordenite (M), and ZSM-5 were studied by fast atom bombardment mass spectrometry (FABMS). Correlations between surface Si^+/Al^+ and bulk Si/Al were established. The surfaces of zeolites were found to be very readily dealuminated by acidic solutions. Analysis of zeolites treated in steam at 600 °C, or reacted with $SiCl_4$ at 500 °C, revealed surface layers enriched in aluminum.

Introduction

The framework composition of zeolite aluminosilicates is an important factor in their physical and catalytic properties.[1,2] Catalytic reactions are particularly dependent upon surface properties and it is important to be able to detect differences between surface and bulk composition. The degree of homogeneity within zeolite crystals is also of interest in the study of zeolite synthesis, ion exchange, sorption, coking, etc.

In recent years several surface analysis techniques have been developed and some have been used to study zeolites. Tempere, Delafosse, and Contour[3] used X-ray photoelectron spectroscopy (XPS) to study the surface composition of zeolites. These authors reported that the surfaces of zeolites A, X, Y, and mordenite (as synthesized in the Na form) were somewhat deficient in aluminum. Deficiency in surface aluminum was more evident in the H form of mordenite (Norton Zeolon) where the ratio Si/Al in the outer surface was 3–5 times larger than that of the bulk. Suib, Stucky, and Blattner[4] studied the surface composition of natural and synthetic zeolites using Auger electron spectroscopy (AES). In contrast to the XPS studies of

† Department of Chemistry, University of Nanjing, Nanjing, People's Republic of China.

(1) Barthomeuf, D. "Studies in Surface Science and Catalysis"; Imelik, B., et al., Eds. Elsevier: Amsterdam, 1980; Vol. 5, p 55.
(2) Abbas, S. H.; Al-Dawood, T. K.; Dwyer, J.; Fitch, F. R.; Georgopoulos, A.; Machado, F. J.; Smyth, S. M. In ref 1, p 27.
(3) Tempere, J., Fr.; Delafosse, D.; Contour, J. P. *ACS Symp. Ser.* **1977**, *No. 40*, 76.
(4) Suib, S. L.; Stucky, G. D.; Blattner, R. J. *J. Catal.* **1980**, *65*, 174.

0022-3654/82/2086-4574$01.25/0